Article

Fluorescence Quantum Yields and Lifetimes of Aqueous Natural Dye Extracted from *Tradescantia pallida purpurea* at Different Hydrogen Potentials

Sthanley R. De Lima, Larissa R. Lourenço, Marina Thomaz, Djalmir N. Messias, Acácio A. Andrade and Viviane Pilla *

Instituto de Física, Universidade Federal de Uberlândia—UFU, Av. João Naves de Ávila 2121, Uberlândia 38400-902, MG, Brazil
* Correspondence: vivianepilla@ufu.br

Abstract: In this work, we monitored the fluorescence quantum efficiency (η) and the fluorescence lifetime (τ) of natural dye extracts from the leaves of *Tradescantia pallida purpurea.* The natural dye was extracted from leaves in aqueous solutions as a function of the potential of hydrogen (pH). The η was determined from conical diffraction (CD) pattern measurements due to thermally-driven self-phase modulation. The fluorescence spectra and time-resolved fluorescence measurements corroborate the CD results, and the average $\eta \approx 0.28$ and $\tau \approx 3.1$ ns values were obtained in the pH range 3.96–8.02. In addition, the extracted natural dye was tested as a possible colorimetric and/or fluorometric pH indicator in milk.

Keywords: natural dye; thermal effects; fluorescence quantum yield; time-resolved spectroscopy; fluorescence; pH indicator

1. Introduction

The growing concern about the environment and the health of the population has expanded the search for more sustainable, natural, and healthy products [1–4]. Natural dyes have gained the attention of both consumers and researchers due to their potential antioxidant, anticarcinogenic, antimicrobial, fungicidal, biochemical, and pharmacological effects, and due to their biodegradable and renewable sources [5–8]. Moreover, the use of synthetic dyes has some disadvantages, such as the possibility of carcinogenic agents, water pollution during the dyeing process, non-renewable sources, and degradation time [9–12].

Anthocyanin is an important source of natural colorant and this dye has been extracted from different plants, flowers, fruits, and tubers [5,13,14]. Anthocyanins are derived from the flavonol compounds with the basic structure of a flavylium ion ($C_{15}H_{11}O^+$), or anthocyanidins that do not have glycated groups [14]. Anthocyanidins consist of a substance with an aromatic ring (A) that is attached to a heterocyclic ring (C). Ring (C) has oxygen, which is responsible for making a carbon–carbon bond to a third aromatic ring (B) [14,15]. When anthocyanidins are found in their glycosylated form, they are called anthocyanins [14]. Anthocyanins strongly absorb the visible region of the electromagnetic spectrum, generating a variety of colors in plants such as red, blue, and purple, according to the different patterns of hydroxyl and methoxyl groups that are attached to the aromatic ring (B), and the sugars and acylated sugars [14–16]. Furthermore, anthocyanins have a wide field of applications in health, such as suppression of neuroinflammation, neuronal degradation, and brain aging [17]. These natural dyes also hold promise in preventing diseases such as cancer [18], cardiovascular illness [19], obesity [20], and diabetes [21], and improving visual health [22] due to the possibility of anthocyanins having antioxidant, antiangiogenesis, and antimicrobial effects [23]. In addition, anthocyanin has the potential

for applications in other areas, such as the pharmaceutical [14], food processing [14], cosmetics manufacturing [24], solar cell development [4], and as pH indicators [25–28].

The possibility of adapting the optical properties of anthocyanins is relevant to the interest in the application of this class of compounds as colorimetric sensors [25–30]. The chemical environment that is involved in anthocyanin extraction causes changes in spectroscopic characterization, stabilization, and thermal parameters, as well as other properties [31]. Currently, the functional mechanism of anthocyanin pigments and their optical characterization is not well understood, despite recent experimental [31–33] and theoretical [34–36] efforts. Therefore, to achieve a better understanding of the optical properties and possible applications, it is necessary to obtain specific spectroscopic and thermo-optical characterizations for the extraction of natural dyes using different solvents. The present work reports on the spectroscopic and optical characterizations of natural dye that was extracted from the leaves of *Tradescantia pallida purpurea* at different values of potential of hydrogen (pH), ranging between 3.96 and 8.02, for bio-applications. The conical diffraction (CD) technique was applied for the determination of fluorescence quantum efficiency (η). Furthermore, for η determination, it is necessary to know the thermo-optical coefficient (dn/dT) of the natural dye. The parameter dn/dT was determined by using the Mach–Zehnder interferometric technique (MZI) [7,37,38]. The fluorescence spectra and time-resolved fluorescence lifetime (TRFL) results were also measured to corroborate the CD results that were obtained for natural dye that was extracted at different pH values. The η parameter plays an important role in studying fluorescent materials and developing new materials for light-emitting devices [39,40]. In addition, the extracted natural dye was tested as a possible probe for milk prepared at different pH values to simulate adulterated food, due to its colorimetric and/or fluorometric properties that change as a function of pH, which allows future use as a possible pH-dependent biosensor [29,30,41].

2. Materials and Methods

2.1. Sample Preparation

Anthocyanin was extracted from the leaves of *Tradescantia pallida purpurea* that were collected from the city of Uberlândia (state of Minas Gerais, Brazil). The process that was carried out to extract the natural dye consisted of washing the leaves with tap and distilled water [7,31] and drying them on absorbent paper. After this, the leaves were cut into small strips and their mass (17 g) was determined by a Shimadzu analytical balance (Model AUW220D, Shimadzu Brazil, SP, Brazil). Next, the leaves were manually macerated at room temperature using a mortar and pestle for approximately twenty minutes with 20 mL of aqueous solution at a specific pH. The homogeneous mixture was then sieved and filtered with paper filter to obtain the dye solution. The aqueous dye was centrifuged for 1.5 h at 7200 rpm (BioPet Model 8011154, Biosigma, SP, Brazil). Then, the samples were stored and refrigerated (~5 °C). A similar procedure was repeated for natural dye extraction in aqueous solutions at different pH values (2.87, 3.66, 5.97, 10.05, 10.30, and 10.80). Distilled water with different concentrations of acetic acid (Sigma-Aldrich) was used for the preparation of acidic solutions, and ammonium hydroxide (NH_4OH) (Synth) was used for the alkaline solutions. The natural dye was tested as a possible pH indicator in whole ultra-high-temperature (UHT) milk (Itambé Alimentos SA, Patos de Minas, Minas Gerais, Brazil) and powdered milk (Nestlé Brasil Ltd.a, Ituiutaba, Minas Gerais, Brazil). The powdered milk samples were prepared using 5 mL of distilled water (at different pH values) and 625 mg of powdered milk. The natural dye (at 0.85 g/mL) was inserted in milk at different pH values, and the samples were homogenized using a magnetic stirrer for 1 h. pH values of 3.47 to 10.43 were used for the natural dye that was inserted in milk that was prepared from powdered milk. A similar procedure was performed using 5 mL of whole UHT milk and natural dye (pH range used between 3.47 and 10.43). Aqueous solutions of natural dye were inserted into the milk samples with different pH values, at a concentration of 40% of natural dye, for fluorescence and lifetime measurements.

2.2. Spectroscopic Techniques

Absorption spectra measurements were performed using a 1 cm quartz cuvette in a portable spectrometer that was equipped with a halogen lamp (Ocean Optics USB2000+, Dunedin, FL, USA) at room temperature. Fluorescence spectra (excitation wavelength at 532 nm) were obtained using a portable spectrometer (DPSSL Driver model MGL532, Midvale, UT, USA). The pH values were determined using an HI 2221 pH meter from Hanna Instruments. Fourier transform infrared (FTIR) spectroscopy was performed using a Perkin–Elmer Frontier spectrometer (resolution of 2 cm^{-1}, PerkinElmer Brazil, SP, Brazil). Time-resolved fluorescence lifetimes (TRFL) were performed by using a light source PLS 450 LED ($\lambda = 460 \pm 10$ nm, 40 µW average power at 40 MHz and 800 ps). TRFL results for liquid samples were analyzed within a FluoTime 100 time-resolved fluorescence spectrometer from PicoQuant (Berlin, Germany) using a 1 cm thick quartz cuvette [41]. A Ludox solution was used as a scattering sample for prompt measurements [41,42].

2.3. Thermo-optical Techniques

2.3.1. Conical Diffraction (CD)

The CD technique takes advantage of the ring pattern that arises due to thermally-induced self-phase-modulation (TSPM) effects [7,37,43,44], behind the cuvette of liquid samples when a relatively high-powered laser beam is focused on a sample. These rings usually emerge when the photothermal phase shift ($\Delta\varphi_{TH}$) that is induced is high enough ($\Delta\varphi_{TH} >> 2\pi$). TSPM effects can be understood as the ability of the excitation beam to induce spatial variations in the refractive index, which leads to a phase shift that depends on the transverse distance from the beam axis [45–47]. For a thermally-induced phase change, the number of rings (N) can be determined in the from [45,48]:

$$N \approx \frac{\varphi \alpha L_{eff} \, P_e}{2\pi K\lambda} \left(\frac{dn}{dT} \right) \qquad (1)$$

where P_e is the power of the excitation laser beam, K is the thermal conductivity, α (cm^{-1}) is the optical absorption coefficient at the excitation wavelength (λ), $L_{eff} = (1 - \exp(-\alpha L))/\alpha$ is the sample effective length, and L is the sample thickness. The fraction of energy that is converted into heat (φ) is related to the fluorescence quantum yield η parameter by the expression [37,43]:

$$\varphi = 1 - \eta \, (\lambda / < \lambda_{em} >) \qquad (2)$$

where $<\lambda_{em}>$ is the average emission wavelength. Here, the CD technique was applied using a linearly polarized argon-ion laser at 514.5 nm that passes through a rotating linear polarizer that is controlled by a step motor to modulate the light intensity. The laser beam, after passing through a focusing lens (f = 20 cm), is folded vertically by a mirror and impinges on a quartz cuvette (2 mm thick) that is placed horizontally [37]. Typical ring patterns were observed when the sample was positioned at the focus of the pump beam due to TSPM effects [37,43–45].

2.3.2. Single Arm Double Interferometer

The refractive index temperature coefficient (*dn/dT*) was determined by using a single-arm double interferometer [37,38]. The Mach–Zehnder interferometric technique (MZI) at a wavelength value of $\lambda = 532$ nm was applied for liquid samples, and *dn/dT* was determined using the expression [37]

$$\frac{dn}{dT} = \lambda/2L\Delta T \qquad (3)$$

where L is the cuvette thickness ($L = 1$ mm) and ΔT is the temperature spacing between two consecutive fringes.

3. Results and Discussion

Figure 1 presents the absorbance spectra and photos of the natural dye solutions that were extracted from the leaves of *Tradescantia pallida purpurea* in different pH values (3.93–8.02). The absorption bands were observed at (508 ± 2), (545 ± 1), and (586 ± 1) nm for all-natural dyes that were extracted in different pH values (Peaks 1, 2, and 3, respectively, as shown in Figure 1). The typical absorbance peaks that were obtained were similar to the results that were reported for the anthocyanin natural dye that was extracted from *Tradescantia pallida* in different solvents as aqueous solutions, sodium citrate buffer (in the pH range of 4–7), ethanol, and acetone [7,31,49,50]. The relationship between absorbance peaks 2 and 3 for the extracted natural dyes as a function of pH are presented in Table 1. The typical absorption bands that were observed in the 500–590 nm region and mainly at 586 nm (peak 3, Figure 1) correspond to B-ring substituted anthocyanins with a quinonoidal base structure [49–51], associated with color stability proprieties due to complex acylation patterns [51]. The pH increases of the aqueous solutions that were used in the natural extraction process promoted a decrease in absorbance peak 2 (Figure 1), as shown in Table 1.
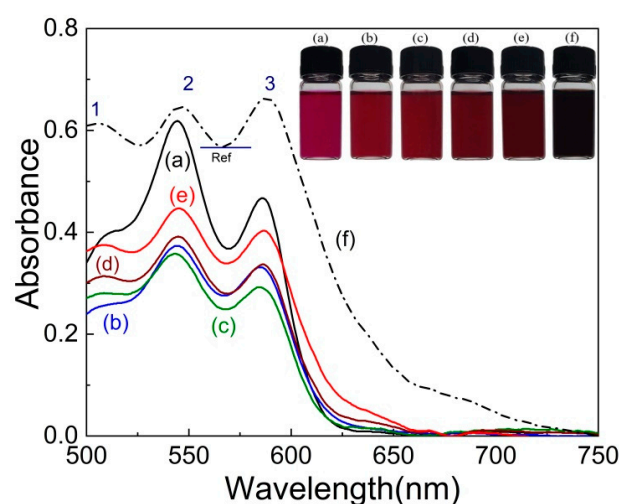

Figure 1. Absorbance and photos of dye that was extracted in aqueous solutions from the leaves of the *Tradescantia pallida purpurea* plant at different pH values: (a) 3.93, (b) 5.28, (c) 5.45, (d) 6.00, (e) 6.83, and (f) 8.02 (concentration of 0.85 g/mL and 2 mm quartz cuvette).

Table 1. The pH values of natural dye solutions that were extracted from *Tradescantia pallida purpurea*. The relationship of absorption peaks used Ref (Figure 1) as a reference, $<\lambda_{em}>$ and Stoke's shift.

Sample	pH (± 0.005)	Peak3/Peak2	$<\lambda_{em}>$ (nm)	Stoke's Shift (nm)
a	3.960	0.394	656	25
b	5.280	0.567	648	24
c	5.450	0.394	652	26
d	6.000	0.514	650	25
e	6.830	0.593	651	23
f	8.020	1.215	655	27

In Zebrina anthocyanin solution (at pH 1.37), it has been reported that the pigment exists only as the flavylium cation, with a maximum wavelength of 537 nm, and when the acidity of the natural dye decreases, the cation is converted to the quinoidal base [49]. The B-ring substituted anthocyanins completely converted to the quinoidal base are reported at pH ~5.5 [49,50]. Another important aspect of anthocyanin to be addressed is the change in its color due to pH, which is due to the ionic nature of the dye structure. In general, at more acidic pH values (pH 1), the structural base of anthocyanins is the flavylium

cation (red color). With a change in pH values, the dye structure becomes a carbinol pseudobase, with quinonoidal and chalcone structures [6,15]. Anthocyanin color (inserted in Figure 1) is reported to be dependent on the structure, pH values, temperature, and other factors [6,15,52]. Furthermore, studies show that anthocyanins can undergo degradation at higher alkaline pH values, depending on the substituent groups that are attached to the structure [6].

Figure 2 presents the fluorescence spectra at an excitation wavelength of λ = 532 nm, for the aqueous dyes that were extracted from the leaves of *Tradescantia pallida purpurea* at different pH values (~3.9–8.0). The values of $<\lambda_{em}>$ and Stoke´s shift wavelength ($\Delta\lambda$) for each natural dye sample (a–f) are presented in Table 1, and the average result for all the natural dye solutions that were extracted in different pH values were $<\lambda_{em}>$ = (652 $\pm$ 3) nm and $\Delta\lambda$ = (25 $\pm$ 1) nm, respectively. The peak emission wavelengths that were obtained were positioned at (611 $\pm$ 2) nm and (648 $\pm$ 1) nm for all natural dyes that were extracted in different pH values. The fluorescence spectra of natural dyes that were extracted from *Tradescantia pallida purpurea* in distilled water and $<\lambda_{em}>$ = 648 nm were reported [7]. The decrease in the fluorescence intensity for more alkaline extractions of the natural dye can be justified due to possible degradation effects [6,52].
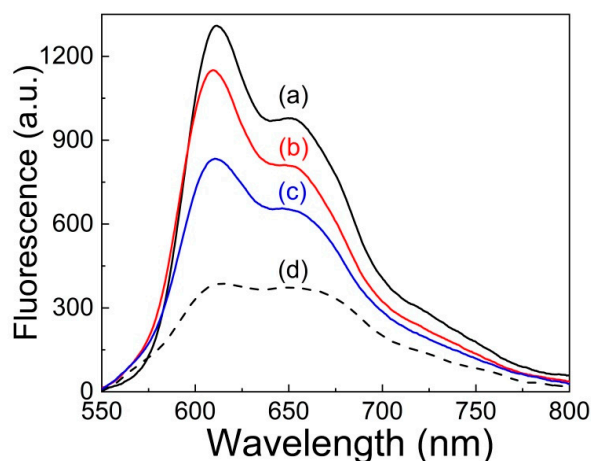

Figure 2. Fluorescence of dyes that were extracted in aqueous solutions from the leaves of the *Tradescantia pallida purpurea* plant at different pH values: (a) 3.96, (b) 5.25, (c) 6.83, and (d) 8.02 (λ = 532 nm, $P_e \approx$ 50 mW, concentration of 0.85 g/mL and 1 cm quartz cuvette).

Fourier-transform infrared (FTIR) spectra for the powder of natural dyes that were extracted in different pH values are presented in Figure 3. The main vibrational modes were observed in the 700–3500 cm^{-1} range at 3187, 1555, 1380, 1085, and 820 cm^{-1} for all the natural dyes in different pH values. For powdered anthocyanin that was extracted in distilled water [7], the main bands that were assigned were reported at 3342 cm^{-1}, attributed to the stretching vibration of hydroxyl (-OH); 1558 cm^{-1}, due to the stretching vibration in the aromatic rings of carbonyl groups (C=C) or (C=O) for anthocyanin dye; and 1081 cm^{-1}, attributed to the C-O-C vibration for anthocyanin dye [7,53,54]. A band at 1380 cm^{-1} belongs to the fingerprint region (1542–965 cm^{-1}), where different IR bands exist due to C-O, C-C, C-H, and C-N bonds [55], and additional bands at 820 cm^{-1} caused by ring vibrations C=C-C [55]. The anthocyanin structure is supported by the presence of these functional groups, such as the benzene ring, double bond, carbonyl group, C-H bond, and OH group [54]. The broad OH peaks are also characteristic of anthocyanin [55]. The discrete band at 3023 cm^{-1} and 2926 cm^{-1}, due to a methyl group (C-H$_3$), can be attributed to aliphatic CH vibrations [55], and with decreasing pH values, peaks at ~3187 cm^{-1} increased, and other peaks at ~3023 cm^{-1} and 2926 cm^{-1} appeared. Similar results were reported for anthocyanin in methanol solution with different pH values, where with the decrease of pH (from 3 to 1), the O-H peak gradually shifted from 3310 cm^{-1} to

3270 cm^{-1} due to the hydroxyl groups of methanol changing into the hydroxyl groups of anthocyanin [56]. The C-O group was detected at 1022 cm^{-1}, and the absorption band in the region of 2950–2840 cm^{-1} can be attributed to the C-H absorption stretching with the sugar group. The peak at 656 cm^{-1}, due to the presence of aromatic C-H bonds, is more apparent when the pH is more acidic [57]. Furthermore, the anthocyanin cyanidin compound has been reported to absorb in the range 3100–3400 cm^{-1} due to O-H, 2900–2840 cm^{-1} due to aliphatic C-H, 675–870 cm^{-1} due to aromatic C-H, and 1660 cm^{-1} due to the presence of aromatic C=C [57,58].
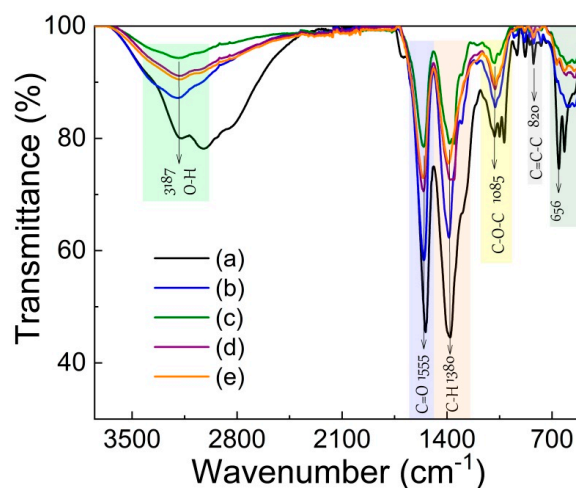

Figure 3. FTIR spectra of natural dye (in powder) that was extracted in different pH values: (a) 3.96, (b) 5.45, (c) 6.00, (d) 6.83, and (e) 8.02.

Natural dyes that were extracted from *Tradescantia pallida purpurea* in aqueous solutions were already analyzed using a high-performance liquid chromatography system coupled with a quadrupole time-of-flight high-resolution mass spectrometer, and the results were described in our Reference [7]. The anthocyanin structures consisted mainly of cyanidin, three glucose molecules, arabinose, and three ferulic molecules [7,59]. Furthermore, the literature reports that the main anthocyanin structures of cyanidin-3,7,3′-triglucosides with three ferulic acid molecules and an additional terminal glucose molecule were obtained from dyes that were extracted from *Tradescantia pallida* leaves [51,60].

Figure 4 shows the results that were obtained using the conical diffraction technique; the number of rings (N) is presented as a function of beam power (P_e). The linear behavior of N versus P_e is presented in the inset of Figure 4, and the slope that was obtained was (18.0 ± 0.5) W^{-1}. The value of φ was determined for the natural dye using Equation (1), the K parameters for aqueous solutions [37], and dn/dT determined using the MZI technique [37,38]. The average value that was obtained for $dn/dT = -(0.92 \pm 0.03) \times 10^{-4}$ K^{-1} (at 22 °C) was in good agreement with the value that was reported in the literature for the pure aqueous solutions [7,37,61]. Using $<\lambda_{em}>$ (Table 1), $\lambda = 514.5$ nm and Equation (2), the radiative quantum yield η values were determined for the all-natural dye samples.

Figure 5 presents the results of φ and η for natural dyes that were obtained from CD as a function of pH. The φ and η results were dependent on the pH of the aqueous solutions that were used for natural dye extractions. The decrease of η (Table 2) for more alkaline solutions can be attributed to the possible degradation [6,52], aggregation, and/or co-pigmentation effects [62,63]. Self-aggregation has been reported for low anthocyanin concentrations [62], and the weakening of their emission efficiency as typically observed in AIE (aggregation-induced emission) active molecules could be due to the activation of non-radiative decay by free molecular rotation [64]. Similar results were obtained for the intensity of fluorescence spectra as a function of pH (Figure 2), which decreased at higher pH values. The η average result for samples at different pH values in the range of (~4.0–8.0) was $\eta = (0.28 \pm 0.02)$. For comparison, for annatto that was extracted from the fruit of the

Bixa Orellana trees at a pH between 5.4 and 11.5, the average value of $\eta = (0.40 \pm 0.08)$ was reported [41], and for the *Carthamus tinctorius* L. petal, $\eta \approx 0.004$ was obtained for the main colored species that was extracted [65].
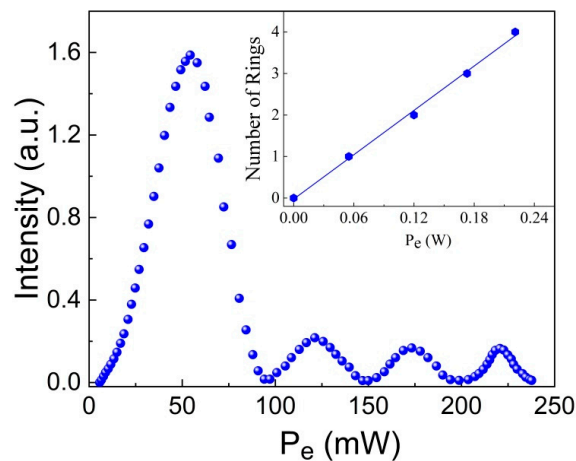

Figure 4. The number of rings (N) as a function of excitation beam power (P_e) for pigment that was extracted from the plant in aqueous solutions ($\alpha = 3.3$ cm^{-1}, pH 5.2, and $\lambda = 514.5$ nm). Inset: *N* versus P_e; the linear trend was obtained by fitting with the slopes of (17.8 ± 0.5) W^{-1} (L = 2 mm).
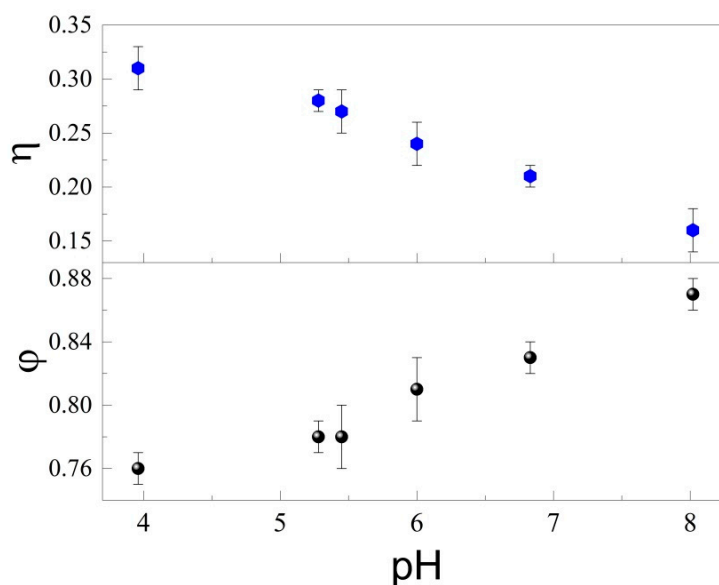

Figure 5. Fluorescence quantum efficiency (η) and absolute nonradiative quantum efficiency (φ) for natural dye that was extracted as a function of pH at 514.5 nm.

Table 2. η, τ, and χ^2 values for aqueous natural dye that was extracted from *Tradescantia* leaves as a function of pH values.

Sample	pH	η	τ (ns)	χ^2
a	3.960	(0.31 ± 0.02)	(3.68 ± 0.06)	(0.99 ± 0.04)
b	5.250	(0.28 ± 0.01)	(3.24 ± 0.05)	(1.11 ± 0.06)
c	5.500	(0.27 ± 0.02)	(3.30 ± 0.06)	(1.15 ± 0.05)
d	6.000	(0.24 ± 0.02)	(3.17 ± 0.06)	(1.11 ± 0.05)
e	6.890	(0.21 ± 0.01)	(2.74 ± 0.04)	(1.10 ± 0.04)
f	8.020	(0.16 ± 0.02)	(2.39 ± 0.03)	(1.07 ± 0.07)

The time-resolved fluorescence (TRFL) spectroscopy measurements were also performed for natural dyes that were extracted in different pH values. TRFL measurements of the excited states were obtained and the experimental results were adjusted using the single exponential A + B × Exp (−t/τ), where A and B are constants, and τ is the fluorescence lifetime. The TRFL setup was tested by using the sodium fluorescein (Synth, molecular weight 376.28) in an alkaline aqueous solution (pH 11.24), and the transient emission was adjusted with a single exponential (τ = (4.13 ± 0.01) ns and χ^2 = (1.03 ± 0.01)) [41,42]. Figure 6 shows the TRFL for aqueous natural dye that was extracted at different pH values (Figure 6 (a) 3.98, (b) 5.34, (c) 6.75, and (d) 7.99) from ornamental leaves of *Tradescantia pallida purpurea*. The fluorescence decays were well fitted with a single exponential, and the χ^2 value was less than 1.15 for all the natural dye aqueous solutions that were extracted as a function of pH (Table 2).
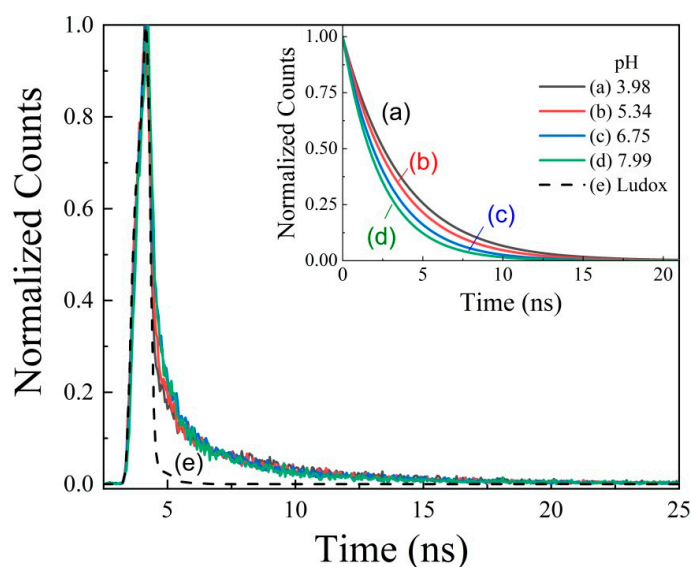

Figure 6. Decay of fluorescence for natural dye that was extracted in different values of pH (a) 3.98, (b) 5.34 (c) 6.75, and (d) 7.99. The values that were obtained for τ were (a) (3.7 ± 0.1), (b) (3.3 ± 0.1), (c) (2.7 ± 0.1), and (d) (2.4 ± 0.1) ns. The decay for Ludox is presented in (e).

The lifetime results that were obtained for aqueous natural dyes are dependent on the pH (Figure 7), with τ increasing for more acidic solutions. A similar dependence on pH was observed for the fluorescence area that was obtained from fluorescence spectra (Figure 7) and η (Figure 5). The average lifetime that was obtained for aqueous anthocyanin dyes that were extracted in different pH values (between ~4 and 8) was (3.1 ± 0.5) ns. The decrease in the fluorescence response generally indicates increased quenching of the emitting center [66], solution degradation, and/or aggregation [6,52,62]. For comparison, the natural dyes from annatto that were extracted from the seeds of the tropical shrub *Bixa Orellana* L. were reported present τ = (1.9 ± 0.3) ns when extracted in aqueous solutions with different pH values (~5.6–11.5), and other typical probes (such as fluorescein, rhodamine 6G, and bacteriochlorophyll), and some fluorescent proteins, present lifetimes in the range of 1–4 ns [41,42,67]. In addition, the fluorescent NIR dye cypate has been reported to present a longer fluorescence lifetime when the pH of the dye changed from a neutral to an acidic value [67].
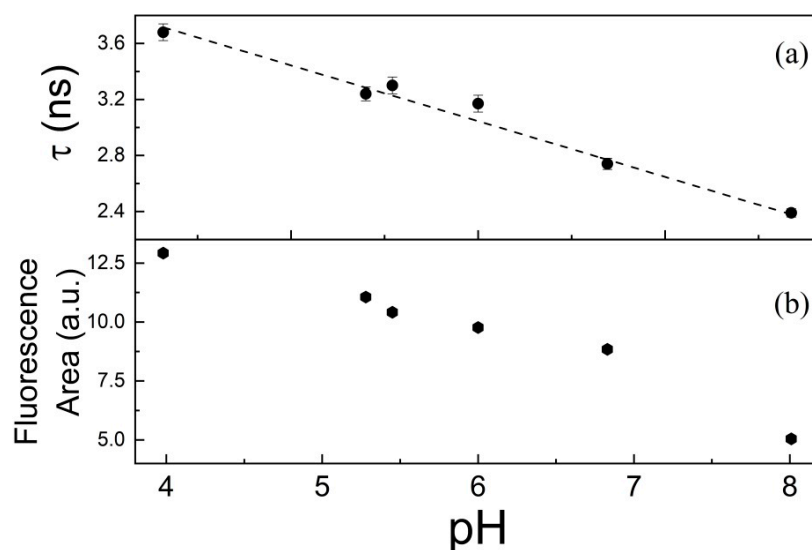
Figure 7. (**a**) Fluorescence lifetime values for natural dye that was extracted as a function of pH at 460 nm, and (**b**) the area of fluorescence spectra (AFS) from measurements that were performed at 532 nm. The dashed adjustment is shown for eye guidance only.

The natural dyes that were extracted from the leaves of *Tradescantia pallida purpurea* were tested as a bioindicator of pH change. Figure 8 shows the fluorescence spectra for anthocyanin (pH 5.450 ± 0.004) inserted in whole UHT milk that was prepared at different pH values (range ~3.47–10.43). The change of the pH in milk was performed to simulate adulterated milk due to bacterial contamination (such as *Mycoplasma bovis* and some *Salmonella serotypes*) [68–70] or other types of contamination, such as urea, starch, water, detergents, caustic soda, and milk from different species [71]. The change in pH values in foods is reported to be due to microbial, chemical, and/or other adulteration actions [30,41,72]. Similar results were obtained for the fluorescence spectra of anthocyanin dye that was inserted into powdered milk at different pH values. The change of the color of the aqueous natural dye that was previously extracted and inserted in milk with different pH values is presented in the photos in Figure 8. For comparison, the results were reported for a natural dye that was extracted from red resin that was removed from the pericarp of annatto seeds [41]. However, in this case, the annatto powder was extracted in milk at different pH values (6.64–10.86) [41]. In comparison with Figure 2, it is possible to observe a change in the fluorescence spectra that is shown in Figure 8. The fluorescence spectra of natural dye that was extracted at different pH values and the anthocyanin that is inserted into milk are different for higher pH values (above ~8). For alkaline pH values, the natural dye fluorescence decreases significantly (Figures 2 and 8), and possible milk fluorescence is predominant.

The TRFL results were performed in anthocyanin that was inserted in milk with different pH values. The fluorescence decays were adjusted with one exponential ($\chi^2 < 1.2$ were obtained for all samples), and the τ results that are presented in Figure 9a were determined from natural dye that was inserted in milk with different pH values. Similar results were obtained for the area of fluorescence spectra (AFS) in the function of the pH-changed milk (Figure 9b). The τ and AFS results as a function of the pH range available between 3.47 and 10.43 are presented in Figure 9a,b, and these parameters changed by ~12 and 50%, respectively. The change in color (inserted in Figure 8) and fluorescence of the anthocyanin-milk samples as a function of pH raises the possibility of using this natural dye as a colorimetric and/or fluorimetric pH-biosensor probe [29,30,41]. Several applications of natural dyes as possible biosensors for adulterated pH-dependent foods have been reported (Table 3) [30,41,72–75]. For applications of natural dyes as possible pH-biosensors, similar behavior of τ and ADF as a pH function were obtained (Figure 9a,b).

However, as a possible parameter for biosensor analysis, the ADF versus pH results could be the simplest technique for implementation.
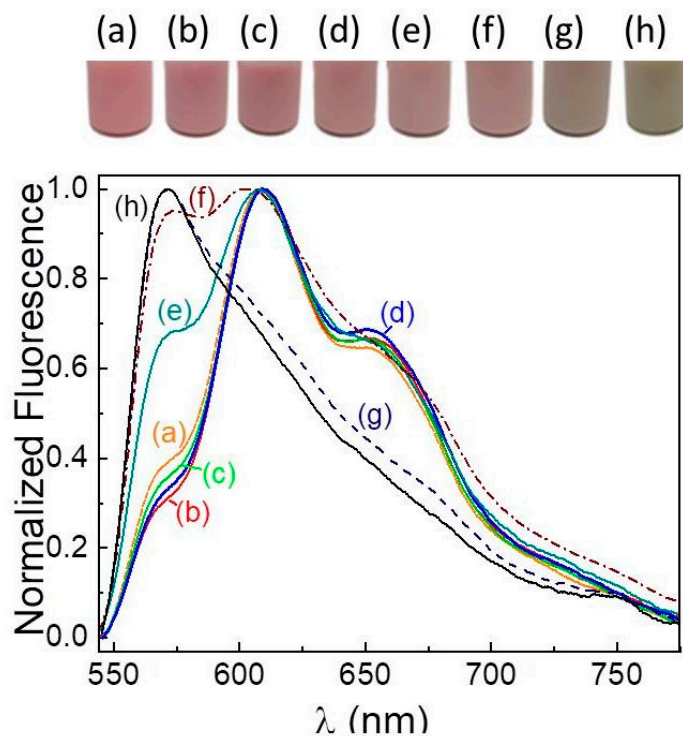

Figure 8. Fluorescence and photos of natural dye that was inserted in milk at different pH values: (a) 3.470, (b) 4.180, (c) 4.980, (d) 6.500, (e) 6.710, (f) 7.950, (g) 8.860, and (h) 10.430 (λ = 532 nm, $P_e \approx 50$ mW, and L = 1 cm).
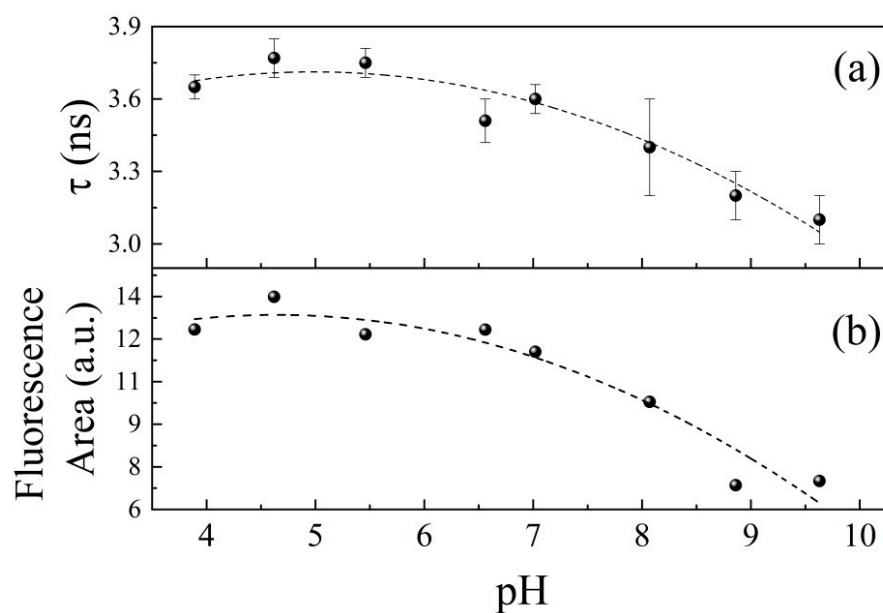

Figure 9. Fluorescence (**a**) lifetime and (**b**) spectra areas (λ = 532 nm, and $P_e \approx 50$ mW) for natural dye that was inserted in milk as a function of the pH value (L = 1 cm). The dashed adjustment is shown for eye guidance only.

Table 3. Applications of natural dyes as pH indicators in foods.

Natural Dye	Extraction	Applications
Anthocyanin	*Brassica oleraceae var. capitata (Red Cabbage)* [73]	Development of chitosan/PVA films doped with anthocyanins to indicate food quality due to pH change. Potential application in the evaluation of milk quality [73].
	Hibiscus rosa-sinensis L. *flowers, Clitoria ternatea flowers, Beta vulgaris roots, Opuntia dillenii pricklypears* [30]	Application of liquid coloring in raw milk to measure microbiological quality control [30].
	Black carrot [72]	Starch film creation with anthocyanin to evaluate milk shelf-life assessment [72].
Curcumin, Quercetin, and Phycocyanin	Vegetable plants, and microalga *Spirulina* [74]	Introduction of natural dyes in nanofibers for use as pH colorimetric indicators as a function of time to monitor food quality [74].
Annatto	Seeds of the shrub *Bixa Orellana* L. [41]	The natural dyes were tested in adulterated milk as colorimetric and/or fluorometric pH-biosensor probes [41].
Litmus	Lichens [75]	Development of a pH-sensing film from polysaccharide extracted from tamarind and litmus lichen, as an indicator of deterioration of cream milk [75].

The natural dye that was extracted from the leaves of *Tradescantia pallida purpurea* was tested in the present work, with a possible colorimetric and fluorometric pH-sensor using different techniques such as AFS, TRFL, and CD. In this case, the aqueous solutions of anthocyanin dye that were previously extracted were inserted in pH-changed milk. The AFS, η, and τ results were obtained with the natural dye that was extracted from the leaves of ornamental plants; these leaves are available in different locations. For comparison, natural dyes that were obtained from annatto seeds were tested as pH sensors in milk [41]. However, in the case of our work [41], the natural dye needed to be extracted in the milk sample at different pH values. The seeds were obtained from the tropical shrub *Bixa Orellana* L., and these trees are restricted to tropical countries.

4. Conclusions

The fluorescence quantum yield (η), the area of fluorescence spectra (AFS), and the fluorescence lifetime (τ) parameters were determined for anthocyanin that was extracted from the leaves of *Tradescantia pallida purpurea* as a function of the potential of hydrogen. The η, AFS, and τ results were dependent on the pH that was used (~3.96–8.02) for aqueous natural dye extraction, with variations of ~48, 50, and 12%, respectively. The effect of extractions of natural dyes at different pH values on photophysical and thermo-optical properties allows the application of anthocyanin dye as a pH-dependent biosensor. Preliminary results are presented for the insertion of aqueous anthocyanin in milk (pH range 3.47–10.43), as a possible colorimetric and fluorometric pH-probe for food.

Author Contributions: Conceptualization, S.R.D.L. and V.P.; methodology, S.R.D.L., L.R.L. and M.T.; formal analysis, S.R.D.L., L.R.L. and V.P.; investigation, S.R.D.L., M.T. and L.R.L.; resources, S.R.D.L., M.T. and L.R.L.; data curation, S.R.D.L., L.R.L. and V.P.; writing—original draft preparation, S.R.D.L., L.R.L. and V.P.; writing—review and editing, S.R.D.L., L.R.L., M.T., D.N.M., A.A.A. and V.P.; supervision, V.P. All authors have read and agreed to the published version of the manuscript.

Data Availability Statement: Not applicable.

Conflicts of Interest: The authors declare no conflict of interest.

References

1. Strobel, G.; Daisy, B.; Castillo, U.; Harper, J. Natural Products from Endophytic Microorganisms. *J. Nat. Prod.* **2004**, *67*, 257–268. [CrossRef] [PubMed]
2. Ghasemlou, M.; Daver, F.; Ivanova, E.P.; Adhikari, B. Bio-inspired Sustainable and Durable Superhydrophobic Materials: From Nature to Market. *J. Mater. Chem. A* **2019**, *7*, 16643. [CrossRef]
3. Balandrin, M.F.; Klocke, J.A.; Wurtele, E.S.; Bollinger, W.H. Natural Plant Chemicals: Sources of Industrial and Medicinal Materials. *Science* **1985**, *228*, 1154–1160. [CrossRef]
4. Blaszczyk, A.; Joachimiak-Lechman, K.; Sady, S.; Tański, T.; Szindler, M.; Drygata, A. Environmental Performance of Dye-Sensitized Solar Cells Based on Natural Dyes. *Sol. Energy* **2021**, *215*, 346–355. [CrossRef]
5. Bendokas, V.; Skemiene, K.; Trumbeckaite, S.; Stanys, V.; Passamonti, S.; Borutaite, V.; Liobikas, J. Anthocyanins: From Plant Pigments to Health Benefits at Mitochondrial Level. *Crit. Rev. Food Sci. Nutr.* **2020**, *60*, 3352–3365. [CrossRef] [PubMed]
6. Castañeda-Ovando, A.; Pacheco-Hernández, M.L.; Páez-Hernández, M.E.; Rodríguez, J.A.; Galán-Vidal, C.A. Chemical studies of anthocyanins: A review. *Food Chem.* **2009**, *113*, 859–871. [CrossRef]
7. De Lima, S.R.; Felisbino, D.G.; Lima, M.R.S.; Chang, R.; Martins, M.M.; Goulart, L.R.; Andrade, A.A.; Messias, D.N.; Dos Santos, R.R.; Juliatti, F.C.; et al. Fluorescence quantum yield of natural dye extracted from *Tradescantia Pallida Purpurea* as a function of the seasons: Preliminary bioapplication as a fungicide probe for necrotrophic fungi. *J. Photochem. Photobiol. B* **2019**, *200*, 111631. [CrossRef]
8. Silva, S.; Costa, E.M.; Calhau, C.; Morais, R.M.; Pintado, M.E. Anthocyanin extraction from plant tissues: A review. *Crit. Rev. Food Sci. Nutr.* **2017**, *57*, 3072–3083. [CrossRef]
9. Hallagan, J.B.; Allen, D.C.; Borzelleca, J.F. The safety and regulatory status of food, drug and cosmetics colour additives exempt from certification. *Food Chem. Toxicol.* **1995**, *33*, 515–528. [CrossRef]
10. Bafana, A.; Devi, S.S.; Chakrabarti, T. Azo Dyes: Past, Present and the Future. *Environ. Rev.* **2011**, *19*, 350–370. [CrossRef]
11. Ardila-Leal, L.D.; Poutou-Pinales, R.A.; Pedroza-Rodríguez, A.M.; Quevedo-Hidalgo, B.E. A Brief History of Colour, the Environmental Impact of Synthetic Dyes and Removal by Using Laccases. *Molecules* **2021**, *26*, 3813. [CrossRef] [PubMed]
12. Cragg, G.M.; Grothaus, P.G.; Newman, D.J. Impact of Natural Products on Developing New Anti-Cancer Agents. *Chem. Rev.* **2009**, *109*, 3012–3043. [CrossRef] [PubMed]
13. Francis, F.J.; Markakis, P.C. Food colorans: Anthocyanins. *Crit. Rev. Food Sci. Nutr.* **1989**, *28*, 273–314. [CrossRef] [PubMed]
14. Khoo, H.E.; Azlan, A.; Tang, S.T.; Lim, S.M. Anthocyanidins and Anthocyanins: Colored Pigments as Food, Pharmaceutical Ingredients, and the Potential Health Benefits. *Food Nutr. Res.* **2017**, *61*, 1361779. [CrossRef] [PubMed]
15. Roy, S.; Rhim, J.-W. Anthocyanin Food Colorant and Its Application in pH-Reponsive Color Change Indicator Films. *Crit. Rev. Food Sci. Nutr.* **2020**, *61*, 2297–2325. [CrossRef] [PubMed]
16. Brouillard, R. Chemical Structure of Anthocyanins. In *Anthocyanins as Food Colors*; Markakis, P., Ed.; Academic Press: New York, NY, USA, 1982; pp. 1–40. [CrossRef]
17. Tsuda, T. Dietary Anthocyanin-Rich Plants: Biochemical Basis and Recent Progress in Health Benefits Studies. *Mol. Nutr. Food Res.* **2012**, *56*, 159–170. [CrossRef]
18. Faria, A.; Pestana, D.; Teixeira, D.; de Freitas, V.; Mateus, N.; Calhau, C. Blueberry Anthocyanins and Pyruvic Acid Adducts: Anticancer Properties in Breast Cancer Cell Lines. *Phytother. Res.* **2010**, *24*, 1862–1869. [CrossRef]
19. Rechner, A.R.; Kroner, C. Anthocyanins and Colonic Metabolites of Dietary Polyphenols Inhibit Platelet Function. *Thromb. Res.* **2005**, *116*, 327–334. [CrossRef]
20. Tsuda, T.; Horio, F.; Uchida, K.; Aoki, H.; Osawa, T. Dietary Cyanidin 3-O-β-D-Glucoside-Rich Purple Corn Color Prevents Obesity and Ameliorates Hyperglycemia in Mice. *J. Nutr.* **2003**, *133*, 2125–2130. [CrossRef]
21. Li, D.; Zhang, Y.; Liu, Y.; Sun, R.; Xia, M. Purified Anthocyanin Supplementation Reduces Dyslipidemia, Enhances Antioxidant Capacity, and Prevents Insulin Resistance in Diabetic Patients. *J. Nutr.* **2015**, *145*, 742–748. [CrossRef]
22. Shim, S.H.; Kim, J.M.; Choi, C.Y.; Kim, C.Y.; Park, K.H. *Ginkgo biloba* Extract and Bilberry Anthocyanins Improve Visual Function in Patients with Normal Tension Glaucoma. *J. Med. Food* **2012**, *15*, 818–823. [CrossRef] [PubMed]
23. Genskowsky, E.; Puente, L.A.; Pérez-Alvarez, J.A.; Fernández-López, J.; Muñoz, L.A.; Viuda-Martos, M. Determination of Polyphenolic Profile, Antioxidante Activity and Antibacterial Properties of Maqui [*Aristotelia chilensis* (Molina) Stuntz] a Chilean Blackberry. *J. Sci. Food Agric.* **2016**, *96*, 4235–4242. [CrossRef] [PubMed]
24. Rojo, L.E.; Roopchand, D.E.; Graf, B.L.; Cheng, D.M.; Ribnicky, D.; Fridlender, B.; Raskin, I. Role of Anthocyanins in Skin Aging and UV-Induced Skin Damage. In *Anthocyanins in Health and Disease*; Wallace, T.C., Giusti, M.M., Eds.; CRC Press: Boca Raton, MA, USA, 2013; pp. 309–322. [CrossRef]

25. Ahmad, N.A.; Heng, L.Y.; Salam, F.; Zaid, M.H.M.; Hanifah, S.A. A Colorimetric pH Sensor Based on *Clitoria* sp and *Brassica* sp for Monitoring of Food Spoilage Using Chromametry. *Sensors* **2019**, *19*, 4813. [CrossRef] [PubMed]

26. Riaz, R.S.; Elsherif, M.; Moreddu, R.; Rashid, I.; Hassan, M.U.; Yetisen, A.K.; Butt, H. Anthocyanin-Functionalized Contact Lens Sensors for Ocular pH Monitoring. *ACS Omega* **2019**, *4*, 21792–21798. [CrossRef] [PubMed]

27. Vo, T.-V.; Dang, T.-H.; Chen, B.-H. Synthesis of Intelligent pH Indicative Films from Chitosan/Poly(vinyl alcohol)/Anthocyanin Extracted from Red Cabbage. *Polymers* **2019**, *11*, 1088. [CrossRef] [PubMed]

28. Choi, I.; Lee, J.Y.; Lacroix, M.; Han, J. Intelligent pH Indicator Film Composed of Agar/Potato Starch and Anthocyanin Extracts from Purple Sweet Potato. *Food Chem.* **2017**, *218*, 122–128. [CrossRef]

29. Steinegger, A.; Wolfbeis, O.S.; Borisov, S.M. Optical Sensing and Imaging of pH Values: Spectroscopies, Materials, and Applications. *Chem. Rev.* **2020**, *120*, 12357–12489. [CrossRef]

30. Madushan, R.; Vidanarachchi, J.K.; Prasanna, P.H.P.; Werellagama, S.; Priyashantha, H. Use of Natural Plant Extracts as a Novel Microbiological Quality Indicator in Raw Milk: An Alternative for Resazurin Dye Reduction Method. *LWT- Food Sci. Technol.* **2021**, *144*, 111221. [CrossRef]

31. Mendes, V.; De Lima, S.R.; Torres, J.O.B.; Antunes, A.; Messias, D.N.; Andrade, A.A.; Dantas, N.O.; Zilio, S.C.; Pilla, V. Preliminary spectroscopic and thermo-optical characterization of anthocyanin unpurified crude extracted from *Tradescantia Pallida Purpurea*. *Dyes Pigm.* **2016**, *135*, 57–63. [CrossRef]

32. Trouillas, P.; Sancho-Garcìa, J.C.; De Freitas, V.; Gierschner, J.; Otyepka, M.; Dangles, O. Stabilizing and Modulating Color by Copigmentation: Insights from Theory and Experiment. *Chem. Rev.* **2016**, *116*, 4937–4982. [CrossRef]

33. Sigurdson, G.T.; Robbins, R.J.; Collins, T.M.; Giusti, M.M. Spectral and Colorimetric Characteristics of Metal Chelates of Acylated Cyanidin Derivatives. *Food Chem.* **2017**, *221*, 1088–1095. [CrossRef] [PubMed]

34. Ge, X.; Timrov, I.; Binnie, S.; Biancardi, A.; Calzolari, A.; Baroni, S. Accurate and Inexpensive Prediction of the Color Optical Properties of Anthocyanins in Solution. *J. Phys. Chem. A* **2015**, *119*, 3816–3822. [CrossRef] [PubMed]

35. Timrov, I.; Micciarelli, M.; Rosa, M.; Calzolari, A.; Baroni, S. Multimodel Approach to the Optical Properties of Molecular Dyes in Solution. *J. Chem. Theory Comput.* **2016**, *12*, 4423–4429. [CrossRef] [PubMed]

36. Cacelli, I.; Ferretti, A.; Prampolini, G. Predicting Light Absorption Properties of Anthocyanidins in Solution: A Multi-Level Computational Approach. *Theor. Chem. Acc.* **2016**, *135*, 156. [CrossRef]

37. De Lima, S.R.; Pereira, G.J.; Messias, D.N.; Andrade, A.A.; Oliveira, E.; Lodeiro, C.; Zilio, S.C.; Pilla, V. Fluorescence Quantum Yield Determination of Molecules in Liquids by Thermally Driven Conical Diffraction. *J. Lumin.* **2018**, *197*, 175–179. [CrossRef]

38. Domenegueti, J.F.M.; Andrade, A.A.; Pilla, V.; Zilio, S.C. Simultaneous Measurement of Thermo-Optic and Thermal Expansion Coefficients with a Single Arm Double Interferometer. *Opt. Express* **2017**, *25*, 313–319. [CrossRef]

39. Yang, D.; Wang, H.; Sun, C.; Zhao, H.; Hu, K.; Qin, W.; Ma, R.; Yin, F.; Qin, X.; Zhang, Q.; et al. Development of a High Quantum Yield Dye for Tumour Imaging. *Chem. Sci.* **2017**, *8*, 6322–6326. [CrossRef]

40. Xie, J.-Y.; Li, C.-Y.; Li, Y.-F.; Fei, J.; Xu, F.; Ou-Yang, J.; Liu, J. Near-Infrared Fluorescent Probe with High Quantum Yield and Its Application in the Selective Detection of Glutathione in Living Cells and Tissues. *Anal. Chem.* **2016**, *88*, 9746–9752. [CrossRef]

41. Santos, T.T.S.; Lourenço, L.R.; de Lima, S.R.; Goulart, L.R.; Messias, D.N.; Andrade, A.A.; Pilla, V. Fluorescence Quantum Yields and Lifetimes of Annatto Aqueous Solutions Dependent on Hydrogen Potenatial: Applications in Adulterated Milk. *J. Photochem. Photobiol.* **2021**, *8*, 100080. [CrossRef]

42. Pilla, V.; Gonçalves, A.C.; dos Santos, A.A.; Lodeiro, C. Lifetime and Fluorescence Quantum Yield of Two Fluorescein-Amino Acid-Based Compounds in Different Organic Solvents and Gold Colloidal Suspensions. *Chemosensors* **2018**, *6*, 26. [CrossRef]

43. Pilla, V.; Munin, E.; Gesualdi, M.R.R. Measurement of the Thermo-Optic Coefficient in Liquids by Laser-Induced Conical Diffraction and Thermal Lens Techniques. *J. Opt. A: Pure Appl. Opt.* **2009**, *11*, 105201. [CrossRef]

44. Iwazaki, A.N.; Pilla, V.; Dias, V.M.; Munin, E.; Andrade, A.A. Self-Induced Phase Modulation for Thermo-Optical Characterization of Annatto Extracted Using Different Solvents. *Appl. Spectrosc.* **2011**, *65*, 1393–1397. [CrossRef]

45. Durbin, S.D.; Arakelian, S.M.; Shen, Y.R. Laser-Induced Diffraction Rings from a Nematic-Liquid-Crystal Film. *Opt. Lett.* **1981**, *6*, 411–413. [CrossRef] [PubMed]

46. Liao, Y.; Song, C.; Xiang, Y.; Dai, X. Recent Advances in Spatial Self-Phase Modulation with 2D Materials and its Applications. *Ann. Phys.* **2020**, *532*, 200322. [CrossRef]

47. Pilla, V.; Menezes, L.D.S.; Alencar, M.A.R.; de Araújo, C.B. Laser-Induced Conical Diffraction due to Cross-Phase Modulation in a Transparente Medium. *J. Opt. Soc. Am. B* **2003**, *20*, 1269–1272. [CrossRef]

48. Catunda, T.; Baesso, M.L.; Messaddeq, Y.; Aegerter, M.A. Time-Resolved Z-scan and Thermal Lens Measurements in Er^{+3} and Nd^{+3} Doped Fluoroindate Glasses. *J. Non-Cryst Solids* **1997**, *213–214*, 225–230. [CrossRef]

49. Brouillard, R. Origin of the Exceptional Colour Stability of the *Zebrina* Anthocyanin. *Phytochemistry* **1981**, *20*, 143–145. [CrossRef]

50. Baublis, A.; Spomer, A.; Berber-Jiménez, M.D. Anthocyanin Pigments: Comparison of Extract Stability. *J. Food Sci.* **1994**, *59*, 1219–1221. [CrossRef]

51. Shi, Z.; Lin, M.; Francis, F.J. Anthocyanins of *Tradescantia pallida*. Potential Food Colorants. *J. Food Sci.* **1992**, *57*, 761–765. [CrossRef]

52. Giusti, M.M.; Wrolstad, R.E. Acylated Anthocyanins from Edible Sources and their Applications in Food Systems. *Bioch. Eng. J.* **2003**, *14*, 217–225. [CrossRef]

53. Ramamoorthy, R.; Radha, N.; Maheswari, G.; Anandan, S.; Manoharan, S.; Williams, R.V. Betalain and Anthocyanin Dye-Sensitized Solar Cells. *J. Appl. Electrochem.* **2016**, *46*, 929–941. [CrossRef]

54. Munawaroh, H.; Fadillah, G.; Saputri, L.N.M.Z.; Hanif, Q.A.; Hidayat, R.; Wahyuningsih, S. The Co-Pigmentation of Anthocyanin Isolated from Mangosteen Pericarp (*Garcinia mangostana* L.) as Natural Dye for Dye-Sensitized Solar Cells (DSSC). *IOP Conf. Ser.: Mater. Sci. Eng.* **2016**, *107*, 012061. [CrossRef]

55. Favaro, L.I.L.; Balcão, V.M.; Rocha, L.K.H.; Silva, E.C.; Oliveira, J.M., Jr.; Vila, M.M.D.C.; Tubino, M. Physicochemical Characterization of a Crude Anthocyanin Extract from the Fruits of Jussara (*Euterpe edulis* Martius): Potential for Food and Pharmaceutical Applications. *J. Braz. Chem. Soc.* **2018**, *29*, 2072–2088. [CrossRef]

56. Jiang, X.; Guan, Q.; Feng, M.; Wang, M.; Yang, N.; Wang, M.; Xu, L.; Gui, Z. Preparation and pH Controlled Release of Fe_3O_4/Anthocyanin Magnetic Biocomposites. *Polymers* **2019**, *11*, 2077. [CrossRef]

57. Wahyuningsih, S.; Wulandari, L.; Wartono, M.W.; Munawaroh, H.; Ramelan, A.H. The Effect of pH and Color Stability of Anthocyanin on Food Colorant. *IOP Conf. Ser. Mat. Sci. Eng.* **2017**, *193*, 012047. [CrossRef]

58. Hurst, W.J. Methods of Analysis for Functional Foods and Nutraceuticals. In *Functional Foods & Nutraceuticals Series*; CRC Press: New York, NY, USA, 2002; Book 4.

59. Baublis, A.J.; Berber-Jiménez, M.D. Structural and Conformational Characterization of a Stable Anthocyanin from *Tradescantia pallida*. *J. Agric. Food Chem.* **1995**, *43*, 640–646. [CrossRef]

60. Shi, Z.; Daun, H.; Francis, F.J. Major Anthocyanin from *Tradescantia pallida*: Identification by LSI-MS and Chemical Analyses. *J. Food Sci.* **1993**, *58*, 1068–1069. [CrossRef]

61. Brochard, P.; Grolier-Mazza, V.; Cabanel, R. Thermal Nonlinear Refraction in Dye Solutions: A Study of the Transient Regime. *J. Opt. Soc. Am. B* **1997**, *14*, 405–414. [CrossRef]

62. Pina, F.; Oliveira, J.; de Freitas, V. Anthocyanins and Derivatives are more than Flavylium Cations. *Tetrahedron* **2015**, *71*, 3107–3114. [CrossRef]

63. Houbiers, C.; Lima, J.C.; Maçanita, A.L.; Santos, H. Color Stabilization of Malvidin 3-Glucoside: Self-Aggregation of the Flavylium Cation and Copigmentation with the Z-Chalcone Form. *J. Phys. Chem. B* **1998**, *102*, 3578–3585. [CrossRef]

64. Diana, R.; Panunzi, B.; Tuzi, A.; Piotto, S.; Concilio, S.; Caruso, U. An Amphiphilic Pyridinoyl-hydrazone Probe for Colorimetric and Fluorescence pH Sensing. *Molecules* **2019**, *24*, 3833. [CrossRef] [PubMed]

65. Clementi, C.; Basconi, G.; Pellegrino, R.; Romani, A. *Carthamus tinctorius* L.: A photophysical Study of the Main Coloured Species for Artwork Diagnostic Purposes. *Dyes Pigm.* **2014**, *103*, 127–137. [CrossRef]

66. Zhegalova, N.G.; He, S.; Zhou, H.; Kim, D.M.; Berezin, M.Y. Minimization of Self-Quenching Fluorescence on Dyes Conjugated to Biomolecules with Multiple Labeling Sites via Asymmetrically Charged NIR Fluorophores. *Contrast Media Mol. Imaging* **2014**, *9*, 355–362. [CrossRef] [PubMed]

67. Berezin, M.Y.; Achilefu, S. Fluorescence Lifetime Measurements and Biological Imaging. *Chem. Rev.* **2010**, *110*, 2641–2684. [CrossRef]

68. Parker, A.M.; House, J.K.; Hazelton, M.S.; Bosward, K.L.; Mohler, V.L.; Maunsell, F.P.; Sheehy, P.A. Milk Acidification to Control the Growth of *Mycoplasma Bovis* and *Salmonella* Dublin in Contaminated Milk. *J. Dairy Sci.* **2016**, *99*, 9875–9884. [CrossRef]

69. Karshima, N.S.; Pam, V.A.; Bata, S.I.; Dung, P.A.; Paman, N.D. Isolation of *Salmonella Species* from Milk and Locally Processed Milk Products Traded for Human Consumption and Associated Risk Factors in Kanam, Plateau State, Nigeria. *J. Anim. Prod. Adv.* **2013**, *3*, 69–74. [CrossRef]

70. Almeida, C.; Cerqueira, L.; Azevedo, N.F.; Vieira, M.J. Detection of *Salmonella Enterica* Serovar Enteritidis Using Real Time PCR, Immunocapture Assay, PNA FISH and Standard Culture Methods in Different Types of Food Samples. *In. J. Food Microbiol.* **2013**, *161*, 16–22. [CrossRef]

71. Azad, T.; Ahmed, S. Common Milk Adulteration and Their Detection Techniques. *Int. J. Food Contam.* **2016**, *3*, 22. [CrossRef]

72. Goodarzi, M.M.; Moradi, M.; Tajik, H.; Forough, M.; Ezati, P.; Kuswandi, B. Development of an easy-to-use colorimetric pH label with starch and carrot anthocyanins for milk shelf life assessment. *Int. J. Biol Macromol.* **2020**, *153*, 240–247. [CrossRef]

73. Pereira, V.A., Jr.; de Arruda, I.N.Q.; Stefani, R. Active chitosan/PVA films with anthocyanins from *Brassica oleraceae* (Red Cabbage) as Time–Temperature Indicators for application in intelligent food packaging. *Food Hydrocoll.* **2015**, *43*, 180–188. [CrossRef]

74. Terra, A.L.M.; Moreira, J.B.; Costa, J.A.V.; de Morais, M.G. Development of time-pH indicator nanofibers from natural pigments: An emerging processing technology to monitor the quality of foods. *LWT Food Sci. Technol.* **2021**, *142*, 111020. [CrossRef]

75. Liang, T.; Wang, L. A pH-Sensing Film from Tamarind Seed Polysaccharide with Litmus Lichen Extract as an Indicator. *Polymers* **2018**, *10*, 13. [CrossRef] [PubMed]